

## Feedback-controlled photorefractive two-beam coupling

V. P. Kamenov and K. H. Ringhofer

*Fachbereich Physik der Universität, D-49069 Osnabrück, Federal Republic of Germany*

B. I. Sturman

*Departamento de Física de Materiales, Universidad Autónoma de Madrid, 28049 Madrid, Spain*

J. Frejlich

*Laboratório de Óptica, Instituto de Física, Universidade Estadual de Campinas, 13083-970 Campinas, São Paulo, Brazil*

(Received 26 June 1997)

We show that a certain phase feedback between output and input changes dramatically the characteristics of photorefractive two-beam coupling. The diffraction efficiency of the dynamic phase grating,  $\eta$ , reaches 1 or 0 (depending on the feedback sign) within a finite time for a wide range of experimental parameters. The spatial-temporal behavior of the wave amplitudes is strongly nonlinear and the grating fringes for  $\eta=1$  or 0 are bended but not tilted. The theory elucidates a number of empirical observations and reveals the great potential of active stabilization for applications. [S1050-2947(97)50710-4]

PACS number(s): 42.65.Hw, 42.65.Sf

Photorefractive two-beam configurations, like the one shown in Fig. 1 have already been the subject of many studies [1,2]. It is well known that the complex amplitudes  $R$  and  $S$  of the reference and signal beams experience strong spatial-temporal variations owing to nonlinear coupling via the induced refractive index grating. Accordingly, the amplitude of this grating,  $\mathcal{E}$ , depends strongly on the propagation coordinate  $x$  and the time  $t$ , and the grating fringes are bended. The diffraction efficiency of such a dynamic grating,  $\eta$ , may approach 1 only in exceptional cases.

Recently, it was found empirically [3–5] that introduction of an electronic feedback loop adjusting the phase of the input signal beam modifies considerably the two-beam coupling. When applied to LiNbO<sub>3</sub> crystals with dominating photovoltaic charge transport, the feedback enables one to reach regularly  $\eta=1$  (or 0) and to suppress remarkably the harmful effect of photoinduced scattering [5]. At the same time, the operation of the feedback loop was interpreted in terms of Kogelnik’s theory [6] (that is, assuming a grating of constant amplitude), which fails already for  $\eta \ll 1$  because of strong nonlinear distortions. Therefore the operating nonlinear-optical device remains, actually, a “black box” and the importance of the experimental results on the active stabilization of the photorefractive beam coupling remains unclear.

In this Rapid Communication we formulate the conditions for active stabilization and describe the main characteristics of the alternative nonlinear device, which differ dramatically from the conventional ones. The results obtained provide a sensible theoretical basis for further development of the active stabilization.

We start our analysis from the known nonlinear equations for the wave amplitudes  $R$ ,  $S$  and the grating amplitude  $\mathcal{E}$ ,

$$\frac{\partial}{\partial \xi} R = i \mathcal{E} S,$$

$$\frac{\partial}{\partial \xi} S = i \mathcal{E}^* R, \tag{1}$$

$$\left( e^{i \delta_1} \frac{\partial}{\partial \tau} + 1 \right) \mathcal{E} = e^{i \delta_2} R S^*,$$

where  $\xi$  and  $\tau$  are the dimensionless coordinate and time, and the asterisk means complex conjugation. The variables  $\xi$  and  $\tau$  as well as the characteristic phases  $\delta_1$  and  $\delta_2$  may be expressed in terms of the characteristic photorefractive lengths and time [1,2]. The amplitudes of the reference and signal waves,  $R$  and  $S$ , are also dimensionless. The total dimensionless intensity,  $|R|^2 + |S|^2$ , which does not depend on  $\xi$ , is supposed to be 1. The set (1) has to be solved in the region  $\tau \geq 0$ ;  $0 \leq \xi \leq \xi_0$ , where  $\xi_0$  is the dimensionless crystal thickness.

As applied to LiNbO<sub>3</sub> crystals,  $|\delta_{1,2}| \ll 1$ ,  $\tau \approx t/t_d$ ,  $t_d$  is the dielectric relaxation time,  $\xi = gx$ ,  $\xi_0 = gx_0$ ,

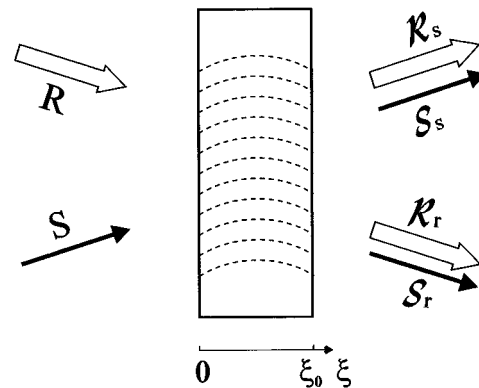


FIG. 1. Schematic of photorefractive two-wave coupling. The bended curves sketch the grating fringes. Vectors  $\mathcal{R}_{s,r}$  and  $\mathcal{S}_{s,r}$  depict decomposing the output waves into transmitted and diffracted ones.

$g \approx \pi n^3 r E_{pv} / \lambda$ ,  $n$  the refractive index,  $r$  the relevant electrooptic constant,  $\lambda$  the wave length,  $E_{pv}$  the photovoltaic field [7], and  $x_0$  is the crystal thickness. For the case of extraordinary waves and  $\lambda = 514$  nm we have a useful numerical relation between  $g$  (measured in  $\text{cm}^{-1}$ ) and  $E_{pv}$  (measured in  $\text{kV/cm}$ ),  $g[\text{cm}^{-1}] \approx E_{pv} [\text{kV/cm}]$ . The photovoltaic field in  $\text{LiNbO}_3:\text{Fe}$  crystals is typically as high as several tens of  $\text{kV/cm}$ . Hence the dimensionless thickness  $\xi_0$  may be considerably greater than 1 even for very thin samples. The characteristic time  $t_d$  is inversely proportional to the total intensity of the incident laser beams. In experiment, it ranges typically from  $10^1$  to  $10^3$  s.

The feedback between the output and the input has to be specified by proper boundary conditions. In order to formulate them one should take into account general properties of the system (1). Its first two equations are linear in  $R$  and  $S$  and do not include time derivatives. These equations describe diffraction of the input reference and signal beams from the refractive-index grating at a moment  $\tau$ . The third equation governs the temporal evolution of the grating amplitude  $\mathcal{E}$ , with a characteristic time  $\sim 1$ . The change of  $\mathcal{E}(\xi, \tau)$  within a time interval  $\delta\tau \ll 1$  is very small.

Let us consider in more detail the diffraction properties of the spatial grating at a moment  $\tau$ . They may be characterized indeed by the amplitudes  $R = R(\xi, \tau)$ ,  $S = S(\xi, \tau)$ , which correspond to the input amplitudes of the recording beams,  $R_0 = R(0, \tau)$ ,  $S_0 = S(0, \tau)$ , but alternatively, these properties may be presented by the fundamental solution  $\mathcal{R}_r$ ,  $\mathcal{S}_r$ , for which  $\mathcal{R}_r(0, \tau) = 1$ ,  $\mathcal{S}_r(0, \tau) = 0$  and by the fundamental solution  $\mathcal{R}_s$ ,  $\mathcal{S}_s$  with  $\mathcal{R}_s(0, \tau) = 0$ ,  $\mathcal{S}_s(0, \tau) = 1$ . These fundamental solutions correspond to testing of the spatial grating, recorded up to the moment  $\tau$ , by only one incident beam (the reference or the signal) of unit amplitude. Using Eqs. (1) it is easy to find that  $\mathcal{S}_s = \mathcal{R}_r^*$ ,  $\mathcal{R}_s = -\mathcal{S}_r^*$  and

$$R = R_0 \mathcal{R}_r + S_0 \mathcal{R}_s, \quad S = R_0 \mathcal{S}_r + S_0 \mathcal{S}_s. \quad (2)$$

The quantity  $\eta = |\mathcal{R}_s(\xi_0, \tau)|^2 = |\mathcal{S}_r(\xi_0, \tau)|^2$  is nothing else than the diffraction efficiency of the grating.

Equations (2) show explicitly that each of the output amplitudes consists of two contributions related to the transmitted and the diffracted waves, respectively; see also Fig. 1. We can therefore consider the phase difference of these components for the output beams  $R$  and  $S$ . For the signal beam this phase difference  $\Phi_s$  is

$$\Phi_s = \varphi_r^0 - \varphi_s^0 + \arg[\mathcal{S}_r(\xi_0)] - \arg[\mathcal{S}_s(\xi_0)], \quad (3)$$

where  $\varphi_s^0$  and  $\varphi_r^0$  are the phases of the input beams,  $\varphi_s^0 = \arg[S_0(\tau)]$ ,  $\varphi_r^0 = \arg[R_0]$ .

The feedback conditions for the active stabilization read

$$\Phi_s = \pm \pi/2. \quad (4)$$

Each of them can be fulfilled by adjusting the input phase  $\varphi_s^0(\tau)$ ; the phase  $\varphi_r^0$  may be put constant. It is important that for any nonzero values  $\mathcal{S}_s(\xi_0)$  and  $\mathcal{S}_r(\xi_0)$ , i.e., for  $\eta(1-\eta) \neq 0$ , each of the  $\pm \pi/2$ -feedback conditions gives only one value of  $\varphi_s^0$  between 0 and  $2\pi$ . If  $\eta$  equals 1 or 0, the feedback fails. As we shall see further, the  $+\pi/2$  feedback leads to  $\eta = 1$ , whereas the  $-\pi/2$  choice leads to  $\eta = 0$ .

In the experiment, adjustment of the input phase  $\varphi_s^0$  was implemented electronically using a modulation technique [1–3]. An additional oscillating component,  $\delta\varphi_s^0 = \psi_d \sin\omega\tau$ ,  $\omega \approx 10^3$ ,  $\psi_d \ll 1$ , was introduced into the phase of the input signal beam. Such a high-frequency modulation does not affect the buildup of the grating and serves for controlling the feedback loop. To modify Eqs. (2), one should replace  $S_0$  by  $S_0 \exp(i\psi_d \sin\omega\tau)$ . As a result, the output intensity  $|S(\xi_0, \tau)|^2$  includes, apart from a constant part, also components oscillating in time as  $\sin\omega\tau$  and  $\cos 2\omega\tau$ . The amplitudes of these components,  $I_\omega$  and  $I_{2\omega}$ , may be represented in the form

$$I_\omega = 2|R_0 S_0| \sqrt{\eta(1-\eta)} \psi_d \sin\Phi_s,$$

$$I_{2\omega} = 0.5|R_0 S_0| \sqrt{\eta(1-\eta)} \psi_d^2 \cos\Phi_s. \quad (5)$$

Using  $I_{2\omega}$  as an error signal and controlling the sign of  $I_\omega$  one can keep  $\Phi_s = \pi/2$  (or  $-\pi/2$ ) till  $\eta(1-\eta) \neq 0$ . The above analysis shows that the feedback conditions for the active stabilization can be implemented without any particular assumptions about the spatial structure of the refractive index grating.

Now we turn to an analysis of the effect of the feedback. First we obtain three exact relations clarifying the effect of the feedback. As follows from Eqs. (2) and (4),

$$\eta = \frac{1}{2} \left( 1 - \frac{W_{\xi_0}}{W_0} \right), \quad (6)$$

where  $W_0$  and  $W_{\xi_0}$  are the input and output values of the intensity difference  $W = |R|^2 - |S|^2$ . Equation (6) shows that  $W_{\xi_0}$  can vary only from  $W_0$  to  $-W_0$  and that the values  $\eta = 0$  and 1 correspond to  $W_{\xi_0} = W_0$  and  $-W_0$ , respectively. Expressing further the product  $S_0 \mathcal{S}_s R_0^* \mathcal{S}_r^*$  through  $R$  and  $S$  with the help of Eqs. (3) and taking into account Eqs. (4) and (6), we get

$$\begin{aligned} \sin\Phi_\Sigma &= \pm \frac{1}{|W_0|} \sqrt{\frac{W_0^2 - W_{\xi_0}^2}{1 - W_{\xi_0}^2}}, \\ \cos\Phi_\Sigma &= \frac{W_{\xi_0}}{W_0} \sqrt{\frac{1 - W_0^2}{1 - W_{\xi_0}^2}}, \end{aligned} \quad (7)$$

where  $\Phi_\Sigma = \varphi_s(\xi_0) + \varphi_r(\xi_0) - \varphi_s(0) - \varphi_r(0)$ . One sees that variations of  $\Phi_\Sigma$  are restricted to the interval  $[0, \pi]$  for the case  $\Phi_s = \pi/2$  and to the interval  $[\pi, 2\pi]$  for  $\Phi_s = -\pi/2$ . The values  $\eta = 1$  and 0 correspond to  $\Phi_\Sigma = \pi$  and  $2\pi$ , respectively. Note that the characteristics of the reference and signal beams only enter Eqs. (7). Therefore they may be considered as a modification of the feedback conditions (4) useful in the  $R, S$  representation.

The governing equations (1) supplemented by the feedback conditions (4) or (7) admit at least one steady-state solution for any input value  $W_0$ . Each steady state corresponds to a nonzero frequency detuning  $\Omega = \Omega(\xi_0, W_0)$  between the  $R$  and  $S$  beams, i.e., to a phase  $\varphi_s^0$  linearly depending on  $\tau$ . However, the value of  $\eta(\xi_0, W_0)$  in the steady state is generally different from 1 and 0. Figure 2 shows a typical

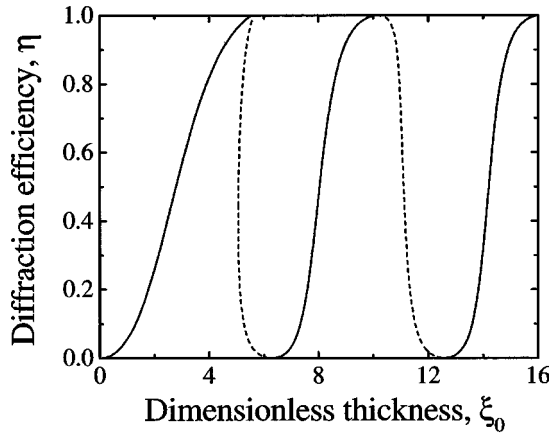


FIG. 2. Dependence  $\eta(\xi_0)$  in the feedback-controlled steady state for  $\delta_1=6.7\times 10^{-3}$ ,  $\delta_2=6.8\times 10^{-2}$ , and  $W_0=0.9$ . The solid parts correspond to  $\Phi_s=\pi/2$ , whereas the dashed ones to  $\Phi_s=-\pi/2$ .

example of the dependence  $\eta(\xi_0)$ . One sees that the diffraction efficiency oscillates between 0 and 1. It is remarkable that the continuous curve  $\eta(\xi_0)$  consists of the parts related to the feedback conditions  $\Phi_s=\pi/2$  and  $-\pi/2$  so that the separating points correspond to  $\eta=1$  and 0. For each particular feedback condition the steady state is possible only within certain intervals of the thickness  $\xi_0$ . Within the interval  $5.0<\xi_0<5.6$  the function  $\eta(\xi_0)$  is multiple-valued. For the case  $\delta_{1,2}=0$ , the points  $\xi_0^{(n)}$  where  $\eta=1$  are given by

$$\xi_0^{(n)} = n\pi + \frac{1}{n\pi} \ln^2 \left( \frac{1+|W_0|}{1-|W_0|} \right) \quad (8)$$

with  $n=1,3, \dots$ , and the points where  $\eta=0$  are simply  $n\pi$  with  $n=2,4, \dots$ .

In order to investigate the temporal development of grating recording, we simulated Eqs. (1) with the feedback conditions (4) and zero initial amplitude  $\mathcal{E}$  for different values  $W_0$  and  $\xi_0$ , and then calculated the corresponding dependences  $\eta(\tau)$ . We have also controlled the correctness of relations (6) and (7). In the calculations we use characteristic phases  $\delta_1=6.7\times 10^{-3}$  and  $\delta_2=6.8\times 10^{-2}$ , typical for  $\text{LiNbO}_3$ . Our results show that in the case  $\Phi_s=\pi/2$  the diffraction efficiency always tends to increase with  $\tau$ . In the region of sufficiently small thickness,  $\xi_0<\xi_0^{(1)}(W_0)$ , the efficiency  $\eta(\tau)$  approaches a value  $\eta_\infty<1$ , which is related to a feedback controlled steady state with  $\Omega\neq 0$ . Outside this region  $\eta$  reaches the value 1 within a finite time. The larger  $\xi_0$  and the smaller  $|W_0|$ , the shorter the transient process. Figure 3 gives representative examples of the described behavior.

In fact, when  $\eta$  reaches a certain value that is very near 1 (the grade of proximity depends on the calculation accuracy), the feedback mechanism ceases to govern the temporal evolution, since an accurate calculation of  $\varphi_s^0$  becomes impossible. In such a case, we keep the phase  $\varphi_s^0$  (or its derivative in  $\tau$ ) equal to the last controllable value. This always results in decreasing  $\eta$ , i.e., makes it possible to return to the feedback mechanism. Each new switching on returns us quickly to a state with  $\eta=1$ , see the inset in Fig. 3.

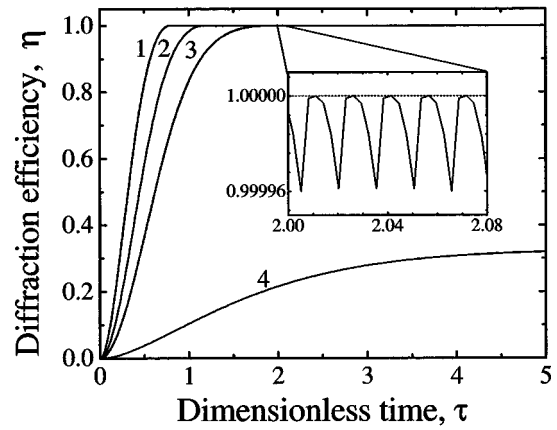


FIG. 3. Dependence  $\eta(\tau)$  for  $\Phi_s=\pi/2$ . The curves 1, 2, 3 correspond to  $\xi_0=6.6$  and  $W_0=0,0.8,0.9$ ; for the curve 4,  $\xi_0=2.2$  and  $W_0=0.9$ . The inset shows in detail the region with  $\eta\approx 1$  for curve 2.

As for the feedback  $\Phi_s=-\pi/2$ , any new switching on makes the grating completely transparent ( $\eta=0$ ) within a finite time. This results in nonsinusoidal oscillations of  $\eta(\tau)$  in the close vicinity of zero (analogous to the oscillations of  $\eta$  near 1 shown in the inset of Fig. 3), irrespective of the thickness  $\xi_0$ .

We have also performed the following numerical experiment. Initially, instead of the feedback we use the boundary condition  $\varphi_s^0=-\Omega_0\tau$  for the input signal beam. The detuning  $\Omega_0$  is chosen in such a way that the temporal evolution brings the system very near to the steady state with  $\Phi_s=\pi/2$  and small  $\eta$ ; see curve 1 in Fig. 4. Then the feedback  $\Phi_s=\pi/2$  is switched on. It is seen that within a finite time the system reaches a state with  $\eta=1$ . A similar numerical experiment was performed by starting from a steady state with  $\Phi_s\approx-\pi/2$  and  $\eta\approx 1$ , switching on the  $-\pi/2$  feedback. It results in a quick drop  $\eta$  to zero; see curve 2 in Fig. 4. We can conclude that the steady state of the system governed by the feedback is generally instable.

One of the most important qualitative characteristics of the photorefractive grating is the form of its fringes. Figure 5

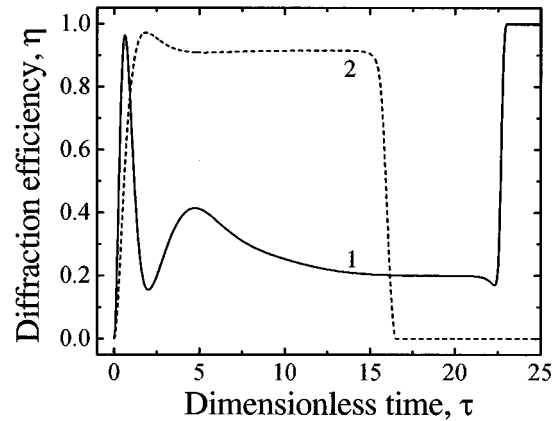


FIG. 4. Up to the point  $\tau=20$  curve 1 corresponds to the input phase  $\varphi_s^0=-\Omega_0\tau$ ,  $W_0=0.5$ ,  $\xi_0=7.3$ . Then the feedback  $\Phi_s=\pi/2$  is switched on. The value  $\Phi_s(20)$  is approximately  $1.01(\pi/2)$ . For curve 2 (dashed) the feedback  $\Phi_s=-\pi/2$  is switched on at  $\tau=13$ ;  $\Phi_s(13)=-1.01(\pi/2)$ ,  $W_0=0.5$ ,  $\xi_0=4$ .

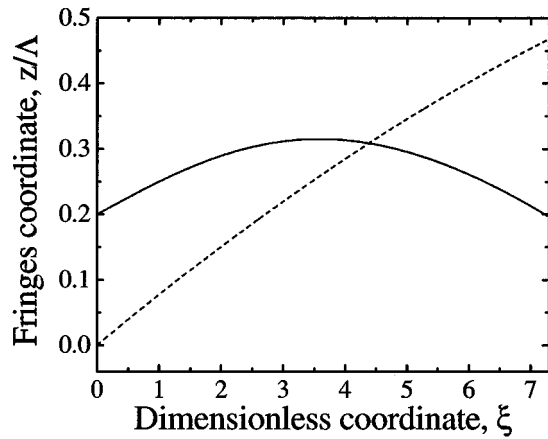


FIG. 5. Fringes of the refractive index grating at the moments  $\tau=20$  (the dashed line) and  $\tau=27$  (the solid line) for the curve 1 in Fig. 4.

shows the fringes of the grating shortly before switching on the  $\pi/2$  feedback (see curve 1 in Fig. 4) and shortly after the moment when  $\eta$  reaches 1. In the first case  $\eta=0.2$  and the fringes are strongly tilted. In the state with  $\eta=1$  the fringes are not tilted but bended. This bending is not strong but not negligible. We have found that for  $\xi_0=6-8$ , the magnitude of bending ranges, depending on  $W_0$ , from 0 to  $0.3\Lambda$ , where  $\Lambda$  is the fringe spacing. Earlier 100% diffractivity was associated exclusively with nonbended gratings.

It is remarkable that some changes of bending persist even after  $\eta$  reaches 1. In other words, there is not one but a whole family of the states with  $\eta=1$  different in the form of the fringes, and also in the spatial profile of  $|\mathcal{E}|$ .

We believe that the above analysis gives an insight into the potential of the feedback controlled photorefractive schemes. In fact, the electronic signal adjusting the input phase  $\varphi_s^0$  may be easily modified to change the phase shift between the output diffracted and transmitted waves to incorporate the effect of light absorption, possible optical activity, etc. It is quite clear that the feedback-controlled photorefractive schemes are less sensitive, in comparison with traditional ones, to low-frequency fluctuations of optical lengths. The advantages of the active stabilization may be very important for the devices based on the photorefractive four-wave mixing [2] and also for fixing of volume holograms [8].

In conclusion, the  $\pm\pi/2$  feedback may be implemented irrespectively of nonlinear photorefractive distortions. It changes dramatically the spatial-temporal characteristics of the photorefractive beam coupling and leads to a state with  $\eta=1$  or 0 within a finite time. The feedback-controlled steady state is generally instable. The active stabilization prevents tilting of the fringes of the refractive-index grating. The electronic feedback loop admits various modifications and is promising for optical devices based on the photorefractive effect.

We would like to thank Volkswagen-Stiftung and INTAS for partial financial support.

[1] P. Yeh, *IEEE J. Quantum Electron.* **25**, 484 (1989).  
 [2] *Photorefractive Materials and Their Applications I*, edited by P. Günter and J.-P. Huignard, *Topics in Applied Physics Vol. 61* (Springer-Verlag, Berlin, 1988), p. 81.  
 [3] A. A. Freschi and J. Frejlich, *J. Opt. Soc. Am. B* **9**, 1837 (1994).  
 [4] P. M. Garcia, K. Buse, D. Kip and J. Frejlich, *Opt. Commun.* **117**, 235 (1995).

[5] P. M. Garcia, A. A. Freschi, J. Frejlich, and E. Krätzig, *Appl. Phys. B* **63**, 207 (1996).  
 [6] H. Kogelnik, *Bell Syst. Tech. J.* **48**, 2909 (1969).  
 [7] B. I. Sturman and F. M. Fridkin, *The Photovoltaic and Photorefractive Effects in Noncentrosymmetric Materials* (Gordon and Breach, Philadelphia, 1992).  
 [8] A. K. Kewitsch, A. Yariv, and M. Segev, in *Photorefractive Effects and Materials*, edited by D. Nolte (Kluwer Academic Publishers, Boston, 1995), p. 173.